Tungsten (2020) 2:289–300
https://doi.org/10.1007/s42864-020-00059-1

Tungsten
www.springer.com/42864

REVIEW PAPER

A review on recent progress of thermionic cathode

Jun-Yan Gao[1] · Yun-Fei Yang[1] · Xiao-Ke Zhang[1] · Shi-Lei Li[1] · Peng Hu[1] · Jin-Shu Wang[1]

Received: 28 June 2020 / Revised: 26 July 2020 / Accepted: 27 July 2020 / Published online: 16 September 2020

Abstract
As the performance of vacuum electron devices is essentially governed by the properties of their cathodes, developing efficient and durable thermionic cathode is necessary and highly desired to meet the boosting requirements of vacuum electron devices. This review summarized the progress made in the past decades with a detailed discussion on the occurred various thermionic cathodes and their features, and the understandings of the correlation between the emission properties and the composition, where structure and synthesis method are well illustrated. Furthermore, dispenser cathodes with novel structures and emission mechanism are highlighted to indicate the recent achievement in this area of research, and Sc-cathode is considered as a promising candidate for the next-generation vacuum electron devices due to the greatly improved efficiency. However, challenges still exist to meet the ever-growing demands of thermionic cathode with collaborative requirement of high performance, easy fabrication and inadequate reproducibility.

Keywords Thermionic cathodes · Performance · Emission mechanism · Ion bombardment · Work function · Tungsten

1 Introduction

As the electron sources for vacuum electron devices (VEDs), thermionic cathodes have been continuously developed and applied in traveling wave tubes (TWTs) [1, 2], magnetrons, communication satellites, medical applications, cathode ray tubes (CRT) [3, 4] and klystrons [5]. Generally, thermionic cathodes use heat to expel electrons from a solid, which is different from cold cathodes using high electric fields to excite electrons out of the solid. The fundamental understanding of the electron emission of thermionic cathodes is that when the activating energy is injected into the cathode metal matrix with increased temperature, the electrons at the Fermi level could capture enough energy to overcome the energy barrier to escape from the cathode surface into the vacuum. According to the Richardson equation [6], energy barrier could be expressed by work function of the cathode materials, and decreasing the work function of cathode surface is a feasible and effective strategy to improve the emission performance. Up to now, many methods to decrease the work function have been developed and thus derived various types of cathodes.

Over the past century, significant progresses have been achieved on thermionic cathodes, and various strategies have been developed to improve their performance with increased power output and source species. The components of cathodes were first developed from pure material to heterogeneous composites, and the traditional mechanical mixing method was replaced by solution synthesis to obtain a uniform structure with enhanced emission efficiency. In addition, chemical-vapor deposition was available to prepare integral active film on the matrix to suppress the peeling off the coating, which results in good stability and prolonged life of cathodes. Furthermore, numerous physical and chemical models are constantly constructed to understand the intrinsical emission mechanism, but the theoretical work still falls behind the technological advancement and needs to be further investigated.

In recent years, rapid development of modern analytical technology endows the ability to comprehending the underlying physical and chemical feature of the emitter process, and theoretical simulation is also available to build the relationship of properties, composition and microstructure

✉ Peng Hu
pengh@bjut.edu.cn

✉ Jin-Shu Wang
wangjsh@bjut.edu.cn

[1] Key Laboratory of Advanced Functional Materials, Education Ministry of China, Faculty of Materials and Manufacturing, Beijing University of Technology, Beijing 100124, China

in details, revealing the nature of cathodes in theory. For instance, atomic force microscopy (AFM) [7] utilizes Van Der Waals Forces between atoms to present the surface properties of the cathode, and photoelectron emission microscopy (PEEM)/thermionic emission microscopy [8] offers the local and relative intensity of electron emission as a function of temperature from the thermionic emission image. Synchronous radiation photoelectron spectrum (SRPES) [9] can provide the in situ surface composition and state evolution during the heating process up to 1200 °C, and the resolution is 3–4 times higher than those of X-ray photoelectron spectroscopy (XPS) and Auger electron spectroscopy (AES). In addition, the density functional theory (DFT) is a theoretical method to investigate the intrinsic emission mechanism by simulating the atomic arrangements, the density of states (DOS), work function, the stability of adsorbates et al. These new approaches greatly enrich the regulation strategies of advanced cathodes and help to improve the electron emission performance which are multiply for specific requirements.

Although significant progress was obtained for thermionic cathodes, few attempts are made to provide a comprehensive summary of their development, and advantages through understanding the recent achievement of thermionic cathodes can provide researchers with different perceptions towards cathode prospect. Accordingly, we systematically summarized the recent development of various thermionic cathodes in this review, and mainly addressed the recent progresses on the emission mechanism, performance and failure of dispenser cathodes. Through reviewing the significant advances on this topic, it may provide new opportunities for designing advanced thermionic cathodes for various applications in vacuum electron devices.

2 Pure material cathodes

2.1 Pure metal cathodes

Pure metals of W, Ta and Re could be used as cathodes, because they can produce thermionic current lower than 1 A·cm^{-2} in operating temperature of above 1727 °C [10]. Among these metals, W attracted noticeable attention in industrial applications due to its high thermal resistance and could deliver a current density of 1.5×10^{-7} A·cm^{-2} with work function of 4.54 eV at 1227 °C [11]. Thus, W-based thermionic cathodes are widely applied in large power concussion machine and electron beam instrument and exhibits the advantages of stable emission and good resistance to ion beam bombardment [12]. However, the ultra-high operating suffers the decreased service life of the heating assembly devices [11], and enhancing the emission ability at low temperature is critical to further widen its applications.

2.2 Compound cathodes

Compound cathodes mainly include carbides and borides [13], and LaB_6 is the mostly representative compound cathode because of its high current density, high resistance to chemical poisoning, good metallic conductivity, low work function and low volatility [14]. The first work on the LaB_6 cathode with work function of 2.66 eV at 1127 °C was reported by Lafferty in 1951 [14], and until 1990, Herniter and Getty [15] achieved the beam current density of 30 A·cm^{-2} at 1744 °C. Later, Ebihara [16] measured a maximum current density of 20 A·cm^{-2} at 1600 °C with an effective work function (Φ) of 2.68 eV, and single-crystal cathode was further developed with an increased current density up to 50 A·cm^{-2} at 1500 °C. Up to now, LaB_6 cathodes are still applied in ionization gauge and mass spectrometer filaments as an electron source with high brightness and high density. However, highly reactive boron would react with refractory metals and further diffuse into the metal lattice to form alloy at elevated temperatures [17], which causes the high instability of the assembled supporter [18]. In recent years, other rare earth boride, such as $La_{0.1}Nd_{0.9}B_6$ [19], $La_{0.4}Pr_{0.6}B_6$ [20] and $Ce_{0.9}Gd_{0.1}B_6$ [21], have been developed, and the largest emission current density reaches 30.65 A·cm^{-2} at 1600 °C.

3 Thoriated tungsten cathodes

Thoriated tungsten cathodes are composed of W and 0.5–2 wt% of thorium oxide, and could deliver an electron emission current ten times higher than that of pure tungsten filament at the same operating condition. Atomic film modeling analysis verified that the greatly improved emission was owing to the formation of a monolayer of free thorium atoms [22] on the surface of tungsten by reduction reaction between thorium oxide and the W_2C layer [10]. The electropositive Th atoms diffuse onto the W surface to form the electric dipole layer during the activation and operation temperature, which facilitates the escape of electrons from the surface due to the decreased work function that depends mainly on the coverage degree of thorium film. Especially, this cathode could operate at 1727 °C with a current density of 2–3 A·cm^{-2} and long stability of 10,000 h [23], respectively, and has been mostly used in the magnetoplasmadynamic (MPD) thruster cathode. However, depletion of the thorium layer would shorten the lifetime of the MPD cathode when the temperature exceeded 2027 °C, and the radioactive pollution of thorium was still a knotty problem needing to be seriously concerned. Therefore, non-radioactive rare earth oxides

(RE_2O_3), such as Y_2O_3 and La_2O_3, have been explored and introduced into the W/Mo cathode to replace ThO_2, and the obtained cathodes exhibit high electron emissivity and low electrode erosion in arc welding [24–26] due to the decrease in the work function [27]. However, the superior stable emission performance of RE_2O_3-W/Mo cathodes were restricted to temperature lower than 1400 °C [26]. Later, a new La_2O_3/Y_2O_3–Gd_2O_3–ZrO_2 composite impregnated W cathode was developed and provided current density of more than 1.5 $A{\cdot}cm^{-2}$ at 1600 °C with a lifetime of 2600 h [28], and are desired to apply in magnetoplasmadynamic thrusters (MPDTs).

4 Oxide cathodes

Oxide cathodes are composed of the mixture of BaO, SrO and CaO as the form of porous layer deposited on pure nickel or tungsten, together with a certain amount of reducing agent (such as Si, Mg). During the thermal activating process, Ba is formed by reduction reaction and diffuses to the surface of oxide particles, and works as activator to promote electron emission. Research work illustrates that the current density of 0.5 $A{\cdot}cm^{-2}$ with work function of 1.5 eV could be obtained at 727 °C for oxide cathodes [10]. At 2012, pulse emission current density dramatically increased to 31 $A{\cdot}cm^{-2}$ manufactured by plasma spray technology [29]. Up to now, oxide cathodes are widely used in receiving tube and TWT [30] due to the easy preparation process, lower operating temperature, longer servicing life and higher electron emission than those of pure metal cathodes [31]. However, challenges still need to be overcome for the oxide cathodes, such as poisoning sensitivity, ohmic heating in the oxide layer [11], and unstable impurities of SiO_2 and MgO, which limit the further applications of the oxide cathodes.

5 Dispenser cathodes

A dispenser cathode consists of a porous metal body in which impregnants including barium oxide, calcium oxide and aluminum oxide are dispensed, and the connected pores also provide channels for active substance to transport to the surface of the cathode [32]. Because of the continuous supply of active substance on the cathode surface, dispenser cathodes exhibit greatly improved emitting performance than that of oxide cathodes and become the most promising cathodes to fulfill the requirements of the VEDs. It should be noted that the rapid diffusion and well distribution of active substance on the surface need to be well addressed and are critical to the emission property of obtained cathodes. Up to now, different dispenser cathodes have been developed and mainly include reservoir cathodes (L-cathodes), impregnated cathodes (B-cathodes), B-cathodes coated with metal film (M-cathodes), mixed matrix cathodes (MM-cathodes) and scandate cathodes (Sc-cathodes).

5.1 L-type cathode

The first dispenser cathode was made by spraying (Ba, Sr) CO_3 onto a nickel base [33, 34], and then (Ba, Sr) CO_3 was developed in a cavity behind porous tungsten. L-cathodes made marked improvements in emission properties such as high emission current capability and long life (more than 100,000 h [35]) at a high loading (>5 $A{\cdot}cm^{-2}$). The high emission of the L-cathode is explained by the formation of an active Ba monolayer on the surface of tungsten by Knudsen flow through the porous channels during thermal activation. However, a barium vapor leak-tight seal between the porous tungsten emitter and the molybdenum support body is very difficult to fabricate, and it is also very hard to keep uniform cathode temperatures due to the low heat transfer efficiency of the cavity [34].

5.2 B-type cathode

The first B-type cathode was produced by impregnating barium aluminate in preformed porous tungsten matrix in 1952 [36], and then calcium oxide was added into the impregnant to decrease the barium loss and generate free Ba active metal when heated, and resulted in the improved emission properties and extended working life [37]. For example, the B-type cathode could decrease emission temperature of 70 °C than the L-cathode with the same cathode current density [10], and the work function of cathode was lowered from 4.6 eV of the W cathode to 2.1 eV [37]. It should be noted the composition of impregnant greatly affect the emission properties of obtained B-type cathode, and molar ratios of BaO, CaO and Al_2O_3 mostly adopted are 5:3:2 [38], 4:1:1 [39] or 6:1:2 [31].

The generally accepted mechanisms for the improved performance are “dipole model” [40] and “excess barium adsorption model” [41] with the emphasized function of active Ba. According to these works, Ba first diffuses from the inside of the matrix to W surface through the pores to form the Ba–O dipole layer at high temperatures, which leads to a sharp decrease of the work function and promotes the electron emission. Continuous Ba supply eliminates the evaporating loss of surface Ba, and the well-preserved Ba film guarantees the excellent current output with enhanced long-time stability. Later, Lu et al. [42] pointed out that oxygen also participated in the activation process to reduce work function. Experimental and theoretical results illustrate that adsorbed oxygen on the tungsten surface not only enhances the Ba–W substrate bonding with strengthened surface dipole, but also dominates the microstructure of cathode

surface, and thus facilitates the decrease of the work-function with enhanced emission capability. In addition, the work function reaches the minimum value when the oxygen concentration is 10^{14} atoms·cm^{-2}, which is mainly attributed to formation of the most stable atomic configuration of Ba–(W, O) complex in the Ba–O–W surface complex. After that, Yin et al. [43] confirmed that absorbed oxygen on cathode surface could oxidize W and Ba atoms after activation by synchronous radiation photoelectron spectrum (SRPS) analysis, and Ba existed in the form of adsorbed chemical compound Ba_mO_n ($m \leq n$) that played an important role in promoting cathode performance.

In recent years, DFT methods were applied to investigate the work function and surface stability of cathodes [40]. Figure 1 presents the adsorbed stability of different species on eight low index surfaces for the W–Ba–O system. Based on the calculation results, $Ba_{0.125}O$ or $Ba_{0.25}O$ are the most thermodynamics favored compounds in the ratio of Ba/O < 1 by passivating each dangling W bond with a single O atom and residing the near Ba. Meanwhile, the work function of the cathode was remarkably decreased to about 2 eV or below, which was consistent with experimental data of the effective work function. Thus, $Ba_{0.125}O$ or $Ba_{0.25}O$ formed on tungsten contribute mostly to the greatly improved performance of B-type cathodes.

The model that combined the work function of different surface grain orientations was further developed, which is calculated according to the area fractions of different surface grain orientations in real polycrystalline W specimens provided via electron backscatter diffraction (EBSD) microscopy [44]. The emitted current density was calculated using Richardson–Dushman equation by DFT and presented as in the form of two-dimensional (2D) map. By adding the empirical Longo-Vaughan, a Miram curve and practical work function distribution (PWFD) curve could be obtained. The experimental work function at the 50% PWFD point was within the range of the DFT/EBSD model prediction, and explored a new strategy to reveal the instinct emission mechanism of thermal cathodes.

5.3 The M-type cathode

M-type cathode was first discovered by Zalm et al. [6] in the late 1960's, in which a noble metal film of Os/Ir/Re/Ru was coated on the surface of impregnated cathodes by a sputtering method. Introducing of the noble metal film endows cathodes about threefold improvement in the emission current density than that of the impregnated cathodes, together with decreased working temperature of about 70–100 °C [33] and good ability to withstand the ion bombardment [45], respectively. For example, the coating Os film and W–Re–Os ternary alloy film could increase the current density to 4.3 A·cm^{-2} and 7.2 A·cm^{-2} at 950 °C$_b$ (brightness temperature), respectively [46], and a current density of 30 A·cm^{-2} with 100,000 h of life operated at 1050 °C$_b$ was acquired for a commercially available M-cathode coated with W–Ru–Os ternary alloy film [47]. Moreover, organometallic Chemical Vapor Deposition (CVD) technique was used to coat B-cathodes with a W–Os alloy film and achieved an excellent emission current density near 50 A·cm^{-2} at 1085 °C$_b$ with 800 h life [48]. Up to now, the M cathode has been confirmed to be the mostly commercially available electrons source for both CRTs and microwave tubes.

Because the work function of noble metals (5.0, 4.8 and 5.3 eV for Re, Os and Ir, respectively) are higher than that of W (4.6 eV) [49, 50], it is quite important to understand the intrinsic mechanism of the improved emission properties of the M-type cathode. Zalm and Van Stratum

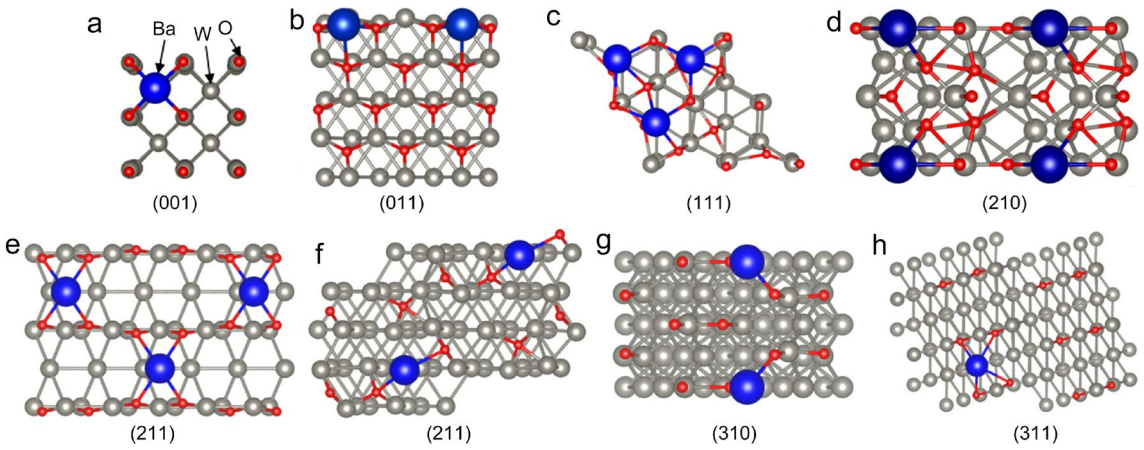

Fig. 1 Surface structures depicting the most stable adsorbed species in the ratio of Ba/O < 1 for the **a** (001), **b** (011), **c** (111), **d** (210), **e** (211), **f** (221), **g** (310), and **h** (311) surface orientations under thermionic cathode operating conditions using the Visualization for electronic and structural analysis (VESTA) code [40]

[6] pointed out the "anomalous effect" to explain this abnormal phenomenon. They stated that the metal film adsorbed on the cathode surface would increase the electronegativity of metal matrix, which reduces energy barrier of surface and provides favorable conditions to reduce work function of W. However, this model is inapplicable to highly electropositive Pt and Au films, because these films did not make any contribution to emission performance. Skinner et al. [51] stated ΔH_{O_2}–ΔH_{Ba} model (ΔH_{O_2}–ΔH_{Ba} is the difference between the heat of sorption of oxygen and barium on the surface) to further explain the specificity of Pt. According to their theory, the low emission properties of Pt and Au are originated from the formation of intermetallic compounds between noble metals and fresh formed Ba reduced from the weaken-bonded BaO. In addition, Yin [49] developed a mechanism about constitution modeling of three chemical states of oxygen to illustrate the improved emission capability by SRPS analysis. As indicated, oxygen underwent state change with temperature increased as shown in Eq. (1). During the activation process, Os oxide (melting point < 500 °C) is decomposed into various low-energy oxygen O^{2-}adsorbed (ads) and increases the amount of adsorbed Ba^{+}, which favors the improvement of emission capability [52]. In addition, the promoting effect of other precious metals (such as Ir and Re) could also be explained by this model, and the decline effect of Pt is attributed to the weak ability to adsorb alkali metals through oxygen on the surface [49]. However, Forman [38] proposed a different point of view that the excellent electron emission of the M-type cathode is depended upon an increased dipole of Os surface covered by Ba rather than the surface concentration of barium according to Auger microprobe spectrometer results.

$$O_2^{2-}(\text{ads}) \rightarrow O^{-}(\text{ads}) \rightarrow O^{2-}(\text{ads}). \quad (1)$$

It is reported that the alloying effect is also responsible to the increased electron emission of cathodes. Green et al. [53] found that a W–Os tetragonal phase σ existed in the Os/W M-type cathode when the Os concentration was between 21 and 35%, and the alloyed compound produced by a reaction between BaO and Os further reduces the chemical potential of Os by possessing populated outer "*d*" orbitals. By virtue of this strategy, some very encouraging results were obtained and after working for 400 h, a half-coated cathode gradually stabilized and delivered a current density of about 1.5 times higher than that of a parallel experimental M-type cathode. Furthermore, an Os–Re–W alloy film was further adopted by adding the Re intermediate layer between W and Os–W films, and exhibited significant improvement of pulsed emission performance of 40 $A{\cdot}cm^{-2}$ at 1102 °C [39]. In addition, the Re intermediate layer also improved the structural stability of alloyed Os–W with well suppressed flaking or peeling during an ageing process.

Besides, the outstanding emission performance of the cathode can also be attributed to the peculiar texture of emitter surface. Balk et al. [54], Li et al. [55] and Swartzentruber et al. [56, 57] pointed that large grains, dense atomic packing, no cracks and stable texture of films contributed to the improved performance and lifetime of cathodes due to the enhanced capabilities against inter-diffusion of W and Os–Ru. In especial, the inter-diffusion increases the W density on cathode surface and in turn decreases the active Os and Ru contents leading to the weakness of the electron emission ability. Moreover, Swartzentruber et al. [58] proved that the existence of the {10–11} texture component devoted to a good performance because the texture altered the knee temperature that is closely related to effective work function.

Furthermore, a new view from energy-level alignment in transition metal oxides was proposed to explain the enhanced emission performance of cathodes [50]. The work function determined by Kelvin probe was located in the range of 5.4 and 5.2 eV for W–Os–Ru ternary alloys with the W concentration varying from 30 to 60 at.%, which is higher than the first ionization energy of 5.2 eV for Ba. The efficient charge transfer from Ba to the substrate is essentially promoted, and produces electric dipole as well as decreased potential energy barrier to favored thermionic emission. Recently, an electron density of states (eDOS)-based theoretical model is developed to qualitatively investigate the electron emitter behaviors [59, 60], and improved thermionic emission could be attributed to a high eDOS just below the Fermi level [61].

5.4 MM cathode

The MM-type cathode was fabricated by modifying the M-cathode through introducing the top layer metals of the M-type cathode into W matrix, and thus offers longer life and higher resistance to ion bombardment than that of M-cathode [62]. This cathode is also known as the mixed-metal matrix cathode since 1970, and possesses low work function (1.98 eV), decreased operational temperature (about 50 K) and improved emission intensity compared with the B-type cathode. For example, Thales W/Os mixed metal matrix cathode exhibits a current density of 5 $A{\cdot}cm^{-2}$ and more than 200 millions of operational hours for space travelling wave tubes [63]. In 2016, a tungsten–osmium matrix hollow cathode with the reservoir technology was successfully adopted in ion engines and Hall thrusters with the current density of 2.5 $A{\cdot}cm^{-2}$ at 910 $°C_b$ and lifetime of 10,000 h, which is 100 °C lower than that of cathodes with tungsten matrices [64]. Compared with the wide applications of M-type cathodes [65], however, MM cathodes are still seldom applied mainly because of some existed limitations. For examples, the W–Ir MM cathode is difficult to fabricate

due to the increased fragility of the compact by adding Ir, and toxic OsO_4 is formed during fabrication and using process for W–Os cathodes.

The emission mechanism of M cathodes is also suitable to the MM cathodes because of the same surface elements of these two kinds of cathodes during thermal emission process. Pankey et al. [66] proposed that a positive Ba–O dipole of monolayer on the Ir surface would decrease the work function of pure Ir. Furthermore, the Ba–O dipoles combining the depolarization model [67, 68] explained the reason of similar lower work function of M- and MM-type cathodes than that of B-type cathodes. According to the depolarization effect of the Ba–O-substrate surface dipole, the work function drops linearly from 4.5 eV for the bare metal substrates to around 2 eV and then increases nonlinearly with the adsorption coverage increasing, where the work function eventually reaches the minimum value. On the other hand, Koch et al. [63] developed a new theoretical model that combined the BaO dipole with a high electrical field to describe the emission mechanism of MM cathodes. According to their work, the reactions of Ba evaporating and oxidizing are occurred at high temperatures and lead to the formation of BaO dipole in front of the W/Os surface [11]. Then, a high electrical field is built up and remarkably decreases the work function due to the decreased Fermi level, which in turn results in the improved electron emission efficiency due to the decreased emission resistance. Recently, we found that the concentration of Ba (Fig. 2a) on the surface of the 75 Re cathode is higher than that of B-type cathodes [69]. Moreover, the small evaporation rates of Ba and BaO (Fig. 2b, c) and the large binding energy of the oxidation state $W^{\delta+}$ (0.2 eV) (Fig. 2d) certify the strong adsorption capacity of Ba and Ba–O on the surface of the 75Re cathode. Furthermore, a higher adsorption energy (about 0.2 eV) of Ba–O and a larger charge transfer of Ba on Re_3W (330) than that on W (110) further confirm the stronger interactions of Ba–O, Ba and matrix by theoretical calculations (Fig. 2e–h). As a result, the mixed matrix cathode possesses a higher ratio of Ba:O [70], more stable Ba–O dipoles on the cathode surface and results in larger emission density than B-type cathodes. Overall, these models confirmed that the noble metals could lower the work function of B-type cathodes through improving the Ba and Ba–O contents on the cathode surface.

5.5 Sc-cathode

Scandia is added either into the tungsten pellet or Ba, Ca aluminate impregnant [71] or top layer [72] to fabricate scandate cathodes since the 1970's [34]. Then researchers paid a lot of effort to increase the electron emission capability by controlling the introducing approaches of Sc and

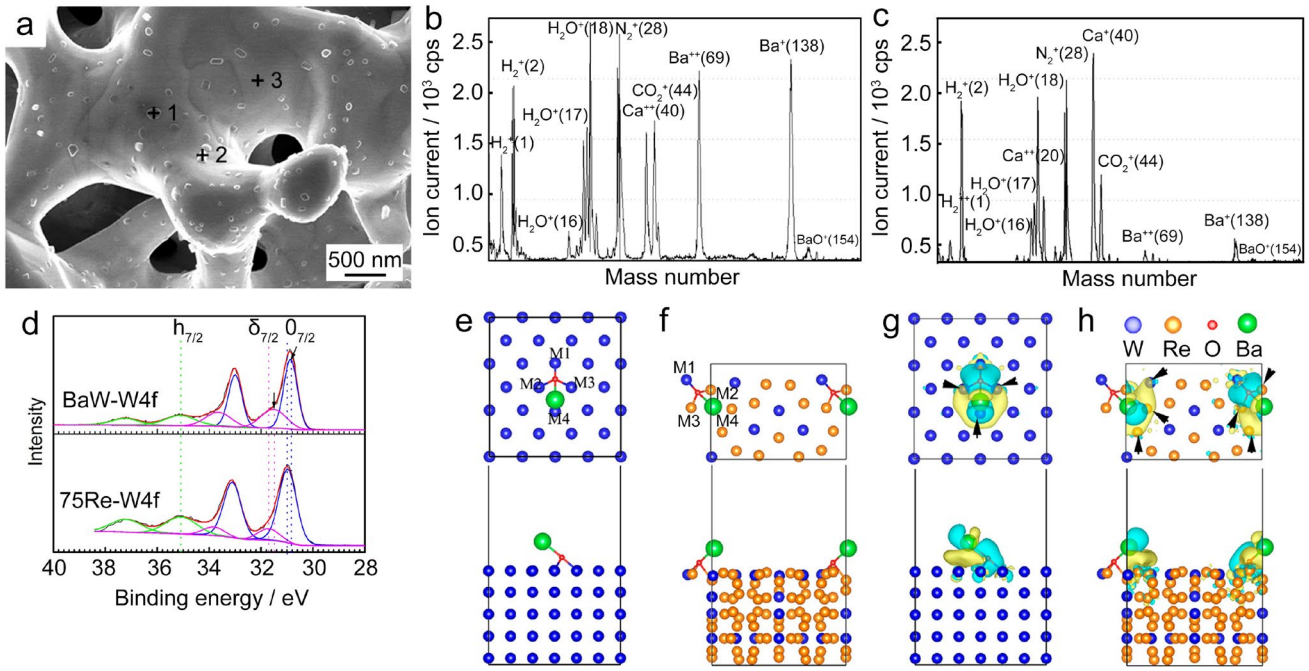

Fig. 2 **a** Micro-morphology of the 75Re cathode after 4 h activation. Time of Flight Mass Spectrometer (TFMS) spectra: **b** Ba–W cathode at 1100 °C_b and **c** 75Re cathode at 1130 °C_b. **d** XPS results for W-4f of the Ba–W cathode and 75Re cathode after 4 h activation. The configuration of the Ba–O dipole adsorbed to the **e** the hollow site of W (110) and **f** hollow site of Re_3W (330). The charge density difference to the **g** W (110) and **h** Re_3W (330), respectively**.** The gaining and losing electrons are represented by yellow and blue colors, respectively Reproduced with permission from Ref. [69]. Copyright 2018 Elsevier

the microstructure of the obtained cathodes, and advanced strategies including the liquid–liquid (L–L) precipitation method, liquid–solid (L–S) precipitation method [73] and pulse laser deposition (PLD) technology [74] are developed to improve the distribution uniformity of the scandium oxide. Up to now, Sc-cathodes have been considered as one of the most potential candidates for the next generation cathodes with high current density [75–77], and could be divided into three different types [45]: the top-layer scandate cathode [72], impregnated scandate cathode (Sc_2O_3 was mixed with Ba–Ca–aluminate impregnant) and scandia-doped dispenser (SDD) cathode [78].

5.5.1 Top-layer scandate cathode

In 1985, Hasker et al. [72] first manufactured the top-layer scandate cathodes by covering W with a film of W-5wt% Sc_2O_3. In comparison, as obtained cathode exhibits a sharply increased thermionic emission current density than that of B- and M-type cathodes owing to the existence of more free Ba and less excess oxygen in the surface by Auger electron spectroscopy analysis [79], and also possesses longer life than that of the pressed scandate cathode and a better recovery after ion bombardment than that of the impregnated scandate cathode [79], respectively. After this work, many methods were developed to prepare top-layer scandate cathodes. For example, Gärtner et al. [80] reported the laser ablation deposition (LAD) of W/Re-Sc_2O_3 on I-cathode substrates, and reveals super high current density of about 400 $A{\cdot}cm^{-2}$ at 965 $°C_b$ and 32 $A{\cdot}cm^{-2}$ at 760 $°C_b$ due to its low work-function of 1.16 eV. Later, Peng et al. [74] used PLD technology to deposit B-type cathode with W + BaO–Sc_2O_3–SrO composite film and received a high current density of 305.5 $A{\cdot}cm^{-2}$. Based on the semiconductor mechanism, they also proposed that the elements interdiffusion among Ba–Sc–Sr–O leads to the formation of active film on the cathode surface, which reduces the work function on the surface of cathodes and in turn improves the emission properties. Uda et al. [81] further investigated emission characteristics of Sc_2O_3/W top-layer scandate cathodes with various layer thicknesses, and pointed out that the thinner Sc_2O_3 layer was favorable for the improvement of current density but negative to the emission stability of cathodes. Accordingly, precise control the thickness of film needs to be seriously concerned to achieve a balance between emission efficiency and lifetime of an obtained top-layer cathode.

5.5.2 Impregnated scandate cathode

The impregnated scandate (I-Sc) cathode was fabricated by impregnating the mixture of BaO, CaO, Al_2O_3 and Sc_2O_3 into the microchannels of porous W body and worked as active substance. Benefiting from this modification, a uniform scandium layer (or tungsten/scandium alloy) on the tungsten surface could be formed by well-dispersed scandium through migration, and exhibits sufficient resistance to ion bombardment [82]. In 1987, Yang et al. [83] prepared barium scandate impregnated dispenser cathode primarily applied in gyrotrons, and the pulse current density reached 20 $A{\cdot}cm^{-2}$ at 850 $°C_b$. In 2003, copper was utilized to fill bars to manufacture porous tungsten body and the recorded stability of 20,000 h was obtained when delivered current densities was 5 $A{\cdot}cm^{-2}$ in Continuous Wave (CW) mode at 950 $°C_b$, while working time with 8000 h was achieved at high current density of 10 $A{\cdot}cm^{-2}$ at 910 $°C_b$ [45]. Up to now, I-Sc-cathodes have been successfully used in a few electron beam devices, such as grid-controlled TWT, mm-wave TWT and klystron in Beijing Vacuum Electronics Research Institute (BVERI) [84].

5.5.3 Scandia-doped dispenser (SDD) cathode

SDD cathodes are produced by impregnating active substance into porous matrix composed of Sc_2O_3 and W, and considered as one of the most promising candidates for the future electron sources. SDD cathodes could be divided into two categories: (1) the scandia-doped impregnated (SDI) cathode and (2) the scandia-doped pressed (SDP) cathode [78]. In the early days, the porous body of SDI cathodes was made by directly sintering of W-Sc_2O_3 mixed powders, and the saturation current density of 10 $A{\cdot}cm^{-2}$ was achieved at 840 $°C_b$ [85]. However, the non-uniform distribution of Sc_2O_3 particles on the cathode surface would weaken the uniformity of the emission current density [82]. To solve this problem, L–L and L–S precipitation methods were employed to introduce Sc_2O_3 into the W matrix, and the current density of more than 30 $A{\cdot}cm^{-2}$ was achieved at 850 $°C_b$ [73]. The cathode prepared by the spray drying method could provide direct current (DC) current density of 30 $A{\cdot}cm^{-2}$ and it could steadily keep for more than 3000 h at 950 °C [86]. It was also found that the machined elliptical impregnated scandate dispenser cathode prepared by a sol–gel technique demonstrated exceeding current–density of 160 $A{\cdot}cm^{-2}$ at 1050 $°C_b$ [82]. For SDP cathode, mixture of barium–calcium aluminate and Sc_2O_3-doped W powders were pressed and sintered to form the cathode [87], and produced a current density of 31.50 $A{\cdot}cm^{-2}$ at 850 °C [88]. Li et al. [89], Cui et al. [90] and Wang et al. [91] further demonstrated that both SDI and SDP cathodes could provide a current density of over 100 $A{\cdot}cm^{-2}$ at 950 $°C_b$.

The improved electron emission in the Sc-cathodes can be attributed to the decreased work function by two reasons: (1) an adsorbed monolayer of Ba–Sc–O on the tungsten surface; (2) semiconductor model. In 2002, Sasaki [92] found that the electron emission of Sc-cathodes is governed by

a certain amount of Sc according to experimental results. Free Sc and free Ba [93] could migrate to the surface of cathode, and the Ba–Sc–O monolayer was formed on the W grains and effectively reduced the work function during activation. On the other hand, Wright et al. [94] developed a semiconductor model for oxide cathodes, and then Raju et al. [95] made a further modification. As indicated, the applied external electric field penetrates the semiconductor surface and forms a layer in the space charge limited area, and the energy levels were then tilted in the semiconductor layer to decrease the work function. Afterwards, Wang et al. [78] developed a more comprehensive statement combining the two above reasons to describe the high emission of SDD cathodes as shown in Fig. 3. First, diffusion of Sc, Ba and O [96] during activation leads to the appearance of a large amount of Ba–Sc–O composite nanoparticles, together with the formation of an active Ba–Sc–O semiconductor layer on the surface of SDD cathodes [97]. Based on the semiconductor model, the external electric field penetrated into the semiconductor surface, and both local electric field and the average emission around nanoparticles were enhanced [97]. Finally, an optimum atomic ratio of Ba/Sc/O with mole ration of (1.5–2):1:(2.0–3.0) was also identified to reach the best emission properties after activating at 1150 $°C_b$ for 1–2 h [78].

Furthermore, Vlahos et al. [98] certified that multicomponent surface coatings also have influence on the work functions of obtained cathodes. According to their work, $Ba_{0.25}Sc_{0.25}O$ with the lowest wok function of 1.16 eV is the most thermodynamically stable phase in $Ba_xSc_yO_z$ alloy that possibly formed on W (001) plane by DFT calculation. The value of work function was also lower than that 1.29 eV of the most stable $Ba_{0.25}O$ structure in Ba–W systems. Therefore, adding Sc promoted the decrease in work functions and is critical to the enhanced emission capability of scandate cathodes.

Kapustin et al. [99] developed a physicochemical mechanism to explain the effect of scandate on the electron emission properties of cathodes. In scandia-doped barium oxide, the disorderly vacancy defects cause the reduction of oxygen vacancy splitting level, and the dipole moment of the system barium vacancy-oxygen vacancy-dopant is significantly enhanced. Thus, additional surface states are formed and markedly decrease the energy band bending near the oxide surface with lowered work function, and further result in a greatly improved emission current. Although there are several assumed conditions existing in the physicochemical model, it is still quite reasonable and could provide a new direction to reveal the intrinsic mechanism of thermionic emission properties.

Liu et al. [100] further explained the mechanism of high emission performance according to the morphological and structural analysis of surface. W grains on the cathode surface are faceted (Fig. 4) and decorated with nanoscale particles composed of BaO (~ 10 nm), $BaAl_2O_4$ and Sc_2O_3 (~ 100 nm) (Fig. 4b–g), respectively, and {112} facets are dominated in all existed facets including {100}, {110} and {112} facets by Wulff analysis. In addition, the strong affinity of Sc for O controls the chemical potential of O with the well establishment of an oxygen-poor atmosphere and favors the formation of Ba_xO_y ($x < y$) adsorbates covered faceted tungsten on cathode surface. According to surface energies of various W facets by DFT calculation [37], $Ba_{0.5}O$ on {112} W facet exhibits the lowest work function of 1.20 eV on W facets and responsible for the greatly improved emission current density.

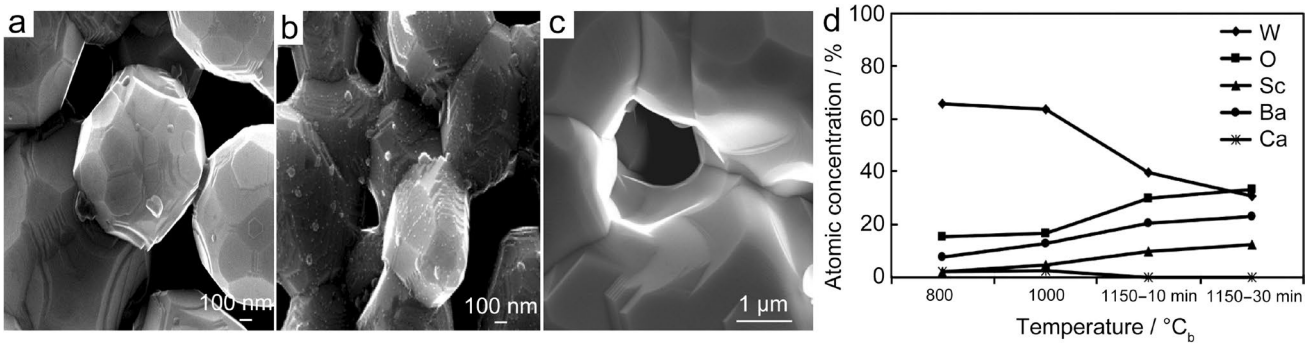

Fig. 3 High-resolution scanning electronic microscopy (SEM) images of SDD cathode **a** after activation and **b** before activation. **c** Morphology of impregnated Ba-type cathodes after activation. Reproduced with permission from Ref. [97]. Copyright 2013 World Scientific Publishing Company. **d** AES surface analysis during cathode activation Reproduced with permission from Ref. [96]. Copyright 2007 IEEE

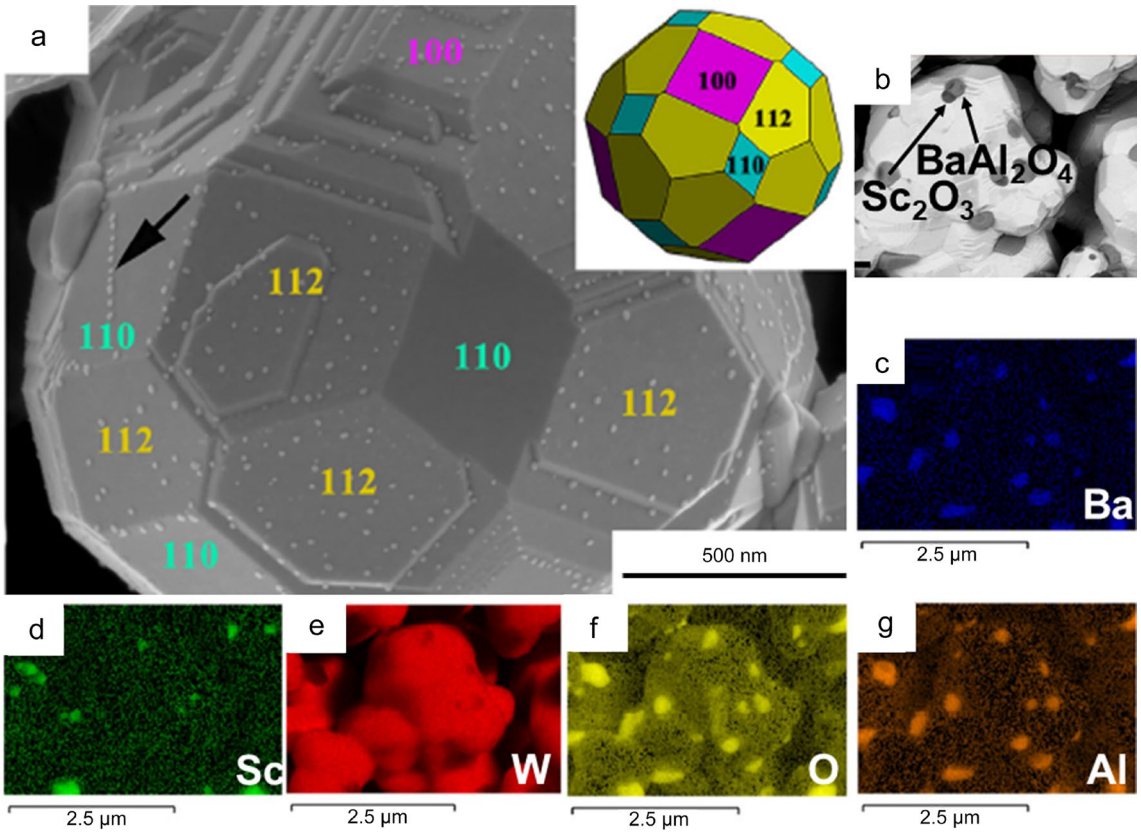

Fig. 4 SEM image of scandate cathodes: **a** W crystal shape constructed from the Wulff analysis; **b** $BaAl_2O_4$ (light gray particles) and Sc_2O_3 (dark gray particles) distributed on W surfaces; **c**–**g** energy-dispersive spectrometer (EDS) elemental map of scandate cathode surface Reproduced with permission from Ref. [100]. Copyright 2019 Elsevier

6 Conclusion

In summary, the latest advance in thermionic cathodes for vacuum electron device applications is reviewed, especially the underlying understanding on the thermionic emission mechanism. Significant progress is achieved from the finding of highly efficient materials to the structure optimization, and the emission efficiency and stability are significantly improved. As a result, the scandate cathode with the outstanding working capability is obtained and considered as the most promising candidate in thermionic cathodes for the future vacuum electron source, but the corresponding emission mechanism is still unclear. Accordingly, the detailed reaction process and continuous scandium production during activation need to be further investigated, which is the key to understand the emission mechanism of cathodes. In addition, more experimental and theoretical work should be conducted, and advanced surface analyzing technologies are highly desired to investigate the emission mechanism. For instance, the in situ detection of the surface component and elemental states during the thermal process are critical to understand the elemental diffusion and redistribution in the real time process. Moreover, the cathodes with high and stable emission performance and good anti-bombarding insensitivity are highly required for the development of new vacuum electron devices, and more attentions and work need to be devoted to the thermionic cathode preparation technique aiming at forming a reliable fabrication technology.

Acknowledgements This work was financially supported by the National Natural Science Foundation of China (Grant No. 51534009) and the Beijing Municipal High Level Innovative Team Building Program (Grant No. IDHT20170502).

References

1. Kornfeld G, Koch N, Harmann H. Development & test status of the thales W/Os mixed metal matrix hollow cathode neutraliser HKN5000. The 29th international electric propulsion conference. Princeton, USA: 2005. p. 298.
2. Windes D, Dutkowski J, Kaiser R, Justice R. Triservice/NASA cathode life test facility. J Appl Surf Sci. 1999;146(1–4):75.
3. Kimura S, Yakabe T, Matsumoto S, Miyazaki D, Yoshii T, Fujiwara M, Koshigoe S. Ir-coated dispenser cathode for CRT. J IEEE Trans Electron Devices. 1990;37(12):2564.
4. Wang J, Yang Y, Wang Y, Liu W, Zhou M, Zuo T. A review on scandia doped tungsten matrix scandate cathode. Tungsten. 2019;1(1):91.

5. Motta CC. Impregnated cathode processing for microwave tubes. 17th IEEE international vacuum electronics conference (IVEC). Monterey, USA. 2016.
6. Zalm P, van Stratum AJA. Osmium dispenser cathodes. Philips Tech Rev. 1966;27:69.
7. Djubua BC, Polivnikova OV. Influence of the dispenser cathodes surface structure on their emission parameters. 10th IEEE international vacuum electronics conference (IVEC). Rome, Italy. 2009. p. 399.
8. Vaughn JM, Jamison KD, Kordesch ME. In situ emission microscopy of scandium/scandium-oxide and barium/barium-oxide thin films on tungsten. IEEE Trans Electron Devices. 2009;56(5):794.
9. Yin S, Yang J, Zhang H. Study on chemical state of oxygen on surface of cathodes coated with Os or W film. IEEE international vacuum electronics conference (IVEC). Bangalore, India. 2011. p. 381.
10. Jenkins RO. A review of thermionic cathodes. Vacuum. 1969;19(8):353.
11. Tuck RA. Thermionic cathode surfaces: the state-of-the-art and outstanding problems. J Vacuum. 1983;33(10–12):715.
12. Wang J, Zhou M, Liu J. Advances in thermionic cathode of tungsten and molybdenum. J Rare Met. 2001;20(3):137.
13. Kosterova NV, Ordan'yan SS, Neshpor VS, Ostrovskii EK. Thermionic emission properties of cermets of eutectic compositions in Me(IV)-(C, B)-(Mo, Re, W) systems. J Sov Powder Metall Met Ceram. 1980;19(1):61.
14. Lafferty JM. Boride cathodes. J Appl Phys. 1951;22(3):299.
15. Herniter ME, Getty WD. High current density results from a LaB_6 thermionic cathode electron gun. IEEE Trans Plasma Sci. 1990;18(6):992.
16. Ebihara K, Hiramatsu S. High-current-density gun with a LaB_6 cathode. Rev Sci Instrum. 1996;67(8):2765.
17. Leung KN, Pincosy PA, Ehlers KW. Directly heated lanthanum hexaboride filaments. Rev Sci Instrum. 1984;55(7):1064.
18. Schmidt PH, Longinotti LD, Joy DC, Ferris SD, Fisk Z. Design and optimization of directly heated LaB_6 cathode assemblies for electron-beam instruments. J Vac Sci Technol. 1978;15(4):1554.
19. Liang CL, Zhang X, Zhang JX, Zhang FZ, Wang Y. Preparation and property of LaNdB cathode material. J Inorg Mater. 2015;30(4):363.
20. Ma RG, Liu DM, Zhou SL, Zhang JX. Fabrication and emission property of polycrystalline $La_{0.4}P_{r0.6}B_6$ bulk prepared by spark plasma sintering. J Inorg Mater. 2010;25(07):73.
21. Wang Y, Zhang X, Zhang JX, Liu HL, Li LL. Excellent thermionic-emission performances of $(Ce_{1-x}Gd_x)B_6$ with ultra-low work functions. J Inorg Mater. 2016;31(8):797.
22. Langmuir I. The electron emission from thoriated tungsten filaments. Phys Rev. 1923;22(4):357.
23. Polk J, Kelly A, Jahn R, Kurtz H, Auweter-Kurtz M. Mechanisms of hot cathode erosion in plasma thrusters. 21st international electric propulsion conference. Orlando, USA. 1990. p. 1.
24. Nakata D, Toki K, Funaki I. Performance of ThO_2-W, Y_2O_3-W and La_2O_3-W cathodes in quasi-steady magnetoplasmadynamic thrusters. J Propuls Power. 2011;27(4):912.
25. NNakata D, Toki K, Funaki I, Shimizu Y, Arakawa Y. Recent study for electrode configuration and material improvement in an MPD thruster. 43rd AIAA/ASME/SAE/ASEE joint propulsionconference & exhibit. Cincinnati, USA. 2007. p. 1.
26. Zhang JX, Zhou M, Zhou WY, Wang JS, Nie ZR, Zuo TY. Thermionic properties of Mo-La_2O_3 cathode wires. Trans Nonferrous Met Soc China. 2002;12(1):43.
27. Chen Z, Zhou ML, Zuo T. Morphological evolution of second-phase particles during thermomechanical processing of W-La_2O_3 alloy. Scr Mater. 2000;43(4):291.
28. Qi SK, Wang XX, Luo JR, Hu MW, Li Y. Rare earth oxide refractory metal salt impregnated W based directly-heated cathode. J Inorg Mater. 2016;031(9):987.
29. Zhang M, Wang XX, L JR, Liao XH. Preparation and emission characteristic study of plasma-sprayed scandia-doped oxide cathode. Acta Physica Sinica. 2012;61(7):468.
30. Liao XH, Wang XX, Zhao QL, Li Y. The application research and development of oxide cathode. J Microw. 2010;S1:534.
31. Fang R, Lu YX. The development of thermionic cathodes. Vac Electron. 2015;1(2):12.
32. Stratum AJAV, Os JGV, Blatter JR, Zalm P. Barium–aluminum–scandate dispenser cathode. US Patent: US4007393 A; 1977.
33. Chopra AK. Impregnated dispenser M-type cathodes for MW tubes—an overview. IETE J Res. 2015;40(1):17.
34. Cronin JL. Modern dispenser cathodes. Commun Speech Vis IEE Proc I. 1981;128(1):19.
35. Vancil BK, Wintucky EG. 2002 Miniature reservoir cathode: an update. International vacuum electron sources conference. Saratov, Russia, 2002. p. 18.
36. Levi R. Improved, "impregnated cathode". J Appl Phys. 1955;26(5):639.
37. Kirkwood DM, Gross SJ, Balk TJ, Beck MJ, Booske J, Busbaher D. Frontiers in thermionic cathode research. IEEE Trans Electron Devices. 2018;65:2061.
38. Forman R. Auger studies comparing the surface concentration of barium on tungsten impregnated and M-cathodes. Appl Surf Sci. 1985;24(3–4):587.
39. Li YT, Zhang HL, Li PK, Zhang MC. Improved performance of the dispenser cathode with a Re intermediate layer. Acta Phys Sin. 2006;55(12):6677.
40. Jacobs R, Morgan D, Booske J. Work function and surface stability of tungsten-based thermionic electron emission cathodes. J Appl Mater. 2017;5(11):116105.
41. Springer RW. Auger electron spectroscopy study of cathode surfaces during activation and poisoning. I. The barium-on-oxygen-on-tungsten dispenser cathode. J Appl Phys. 1974;45(12):5260.
42. Lu QB. New model for the role of oxygen in the emitting surface of the impregnated tungsten cathode. J Int J Electron. 1989;67(4):645.
43. Yin SY, Zhang HL, Ibrahim U, Qian HJ, Wang JO, Wang Y, Wang XX. SRPES study on surface of impregnated barium tungsten cathodes. J Microw. 2010;S1:19.
44. Chen DZ, Jacobs R, Vlahos V, Jensen KL, Morgan D, Booske J. Combining theory and experiment to model electron emission from polycrystalline tungsten cathode surfaces. International vacuum electronics conference. Monterey, CA, 2018. p. 39.
45. Ji L, Yan S, Shao W, Chen Q, Min Z. Investigation and application of impregnated scandate cathodes. Appl Surf Sci. 2003;215(1–4):49.
46. Yin SY, Zhang HL, Ding YG. Manufacturing for high-performance multibeam cathodes. 10th IEEE international vacuum electronics conference (IVEC). Rome, Italy.
47. Mita N. Degradation of coated impregnated cathode's surface coating. IEEE Trans Electron Devices. 1991;38(11):2554.
48. Shih A, Berry A, Marrian CRK, Haas GA. Os-coated cathode for very high emission-density applications. IEEE Trans Electron Devices. 1987;34(5):1193.
49. Yin SY. Experimental and theoretical research of electron emission mechanism of M-type cathodes. J Electron. 2014;31(2):159.
50. Swartzentruber PD, Detisch MJ, Balk TJ. Composition and work function relationship in Os–Ru–W ternary alloys. J Vac Sci Technol A Vac Surf Films. 2015;33(2):021405.
51. Skinner HB, Tuck RA, Dobson PJ. Theoretical models of dispenser cathode surfaces. J Phys D Appl Phys. 1982;15(8):1519.

52. Yin SY, Zhang YQ. Emission mechanism and technical progresses for M-type cathodes. 9th international vacuum electron sources conference (IVESC). Monterey, USA. 2012. p. 467.
53. Green MC, Skinner HB, Tuck RA. Osmium-tungsten alloys and their relevance to improved M-type cathodes. Appl Surf Sci. 1981;8:13.
54. Balk T, Li WC, Roberts S. Characterization of osmium-ruthenium coatings for porous tungsten dispenser cathodes. 9th IEEE international vacuum electronics conference (IVEC). Monterey, USA. 2008. p. 40.
55. Li WC, Roberts S, Balk T. Effects of annealing on microstructure of osmium-ruthenium thin films. 10th IEEE international vacuum electronics conference (IVEC). Rome, Italy. 2009. p. 177.
56. Swartzentruber P, Li WC, Balk T, Roberts S. Optimizing osmium-ruthenium films to inhibit tungsten interdiffusion. IEEE international vacuum electronics conference (IVEC). Monterey, USA. 2010. p. 73.
57. Swartzentruber PD, Balk T, Roberts SJ. Characterization of osmium-ruthenium thin films for cathode coatings. TMS 140th annual meeting and exhibition. San Diego, USA. 2011. p. 613.
58. Swartzentruber PD, Balk TJ, Effgen MP. Correlation between microstructure and thermionic electron emission from Os-Ru thin films on dispenser cathodes. J Vac Sci Technol A. 2014;32(4):040601.
59. Zhou Q, Balk TJ, Beck MJ. Interplay of composition, structure, and electron density of states in W–Os cathode materials and relationship with thermionic emission. J Vac Sci Technol A Vac Surf Films. 2017;35(2):021601.
60. Zhou QF, Balk TJ, Beck MJ. Stable structures and electron density of states of W-Os alloys for dispenser cathodes. 15th IEEE international vacuum electronics conference (IVEC). Monterey, USA. 2014. p. 525.
61. Zhou QF, Balk TJ, Beck MJ. Quantum mechanical investigation of thermionic emission from Os-coated tungsten dispenser cathodes. IEEE international vacuum electronics conference (IVEC). Monterey, CA. 2016.
62. Ravi M, Kumar KS, Bhat KS . Tungsten-rhenium mixed metal matrix cathodes. IEEE international vacuum electronics conference(IVEC). Bangalore, India. 2011. p. 39.
63. Koch N, Harmann H, Kornfeld G. Status of the THALES tungsten/osmium mixed-metal hollow cathode neutralizer development. The 30th international electric propulsion conference. Florence, Italy. 2007. p. 1.
64. Vancil B, Lorr J, Schmidt V, Ohlinger W, Polk J. Reservoir hollow cathode for electric space propulsion. IEEE Trans Electron Devices. 2016;63:4113.
65. Green MC. Cathode technology overview-current status and future direction. 9th IEEE international vacuum electronicsconference (IVEC). Monterey, USA. 2008. p. 3.
66. Pankey T, Thomas RE. Orientation dependence of work function: BaO on Ir. Appl Surf Sci. 1981;8:50.
67. Muller W. Computational modeling of dispenser cathode emission properties. International electron devices meeting(IEDM). Washington, USA. 1992. p. 1441.
68. Zhang HW, Wu HX, He ZC. Emission performance studies of mixed barium-tungsten cathode. Chin J Electron Devices. 2006;30(1):57.
69. Lai C, Wang J, Zhou F, Liu W, den Engelsen D, Miao N. Emission and evaporation properties of 75 at% Re-25 at% W mixed matrix impregnated cathode. Appl Surf Sci. 2018;427:874.
70. Brion D, Tonnerre JC, Shroff A. Electron emission and surface composition of osmium and osmium-tungsten coated dispenser cathodes. Appl Surf Sci. 1985;20:429.
71. Wang J, Wang Y, Tao S, Li H, Yang J, Zhou M. Scandia-doped tungsten bodies for Sc-type cathodes. Appl Surf Sci. 2003;215(1–4):38.
72. Hasker J, Stoffelen HJH. "Alternative" auger analysis reveals important properties of M-type and scandate cathodes. Appl Surf Sci. 1985;24(3–4):330.
73. Yuan H, Gu X, Pan K, Wang Y, Liu W, Zhang K, Wang J, Zhou M, Li J. Characteristics of scandate-impregnated cathodes with sub-micron scandia-doped matrices. Appl Surf Sci. 2005;251(1–4):106.
74. Peng Z, Yin SY, Zheng Q, Wang XX, Li Y. Emission performance of scandate cathodes prepared by pulse laser deposition. J Electron Inf Technol. 2014;36(3):754.
75. Wan C, Kordesch ME. Tungstate formation in a model scandate thermionic cathode. J Vac Sci Technol B. 2012;31(1):1210.
76. Yamamoto S, Taguchi S, Aida T, Kawase S. Study of metal film coating on Sc_2O_3 mixed matrix impregnated cathodes. Appl Surf Sci. 1984;17(4):517.
77. Vancil B, Brodie I, Lorr J, Schmidt V. Scandate dispenser cathodes with sharp transition and their application in microwave tubes. IEEE Trans Electron Devices. 2014;61(6):1754.
78. Wang Y, Wang J, Liu W, Li L, Wang Y, Zhang X. Correlation between emission behavior and surface features of scandate cathodes. IEEE Trans Electron Devices. 2009;56(5):776.
79. Hasker J, Esdonk JV, Crombeen JE. Properties and manufacture of top-layer scandate cathodes. Appl Surf Sci. 1986;26(2):173.
80. Gärtner G, Geittner P, Lydtin H, Ritz A. Emission properties of top-layer scandate cathodes prepared by LAD. Appl Surf Sci. 1997;111:11.
81. Uda E, Nakamura O, Matsumoto S, Higuchi T. Emission and life characteristics of thin film top-layer scandate cathode and diffusion of Sc_2O_3 and W. Appl Surf Sci. 1999;146(1–4):31.
82. Zhao J, Gamzina D, Li N, Li J, Spear A, Barnett LR, Li N, Banducci M, Risbud S, Neville L. Scandate dispenser cathode fabrication for a high-aspect-ratio high-current-density sheet beam electron gun. IEEE Trans Electron Devices. 2012;59(6):1792.
83. Yang LY, Wang SS. Investigation on pulse properties of impregnated barium scandate dispenser cathodes. J Electron. 1987;01:55.
84. Fukuda S, Hayashi K, Maeda S, Michizono S, Saito Y. Performance of a high-power klystron using a BI cathode in the KEK electron linac. Appl Surf Sci. 1999;146(1–4):84.
85. Taguchi S, Aida T, Yamamoto S. Investigation of Sc_2O_3 mixed-matrix Ba–Ca aluminate-impregnated cathodes. IEEE Trans Electron Devices. 1984;31(7):900.
86. Zhu X, Wang Y, Liu W, Yang F, Wang J. Emission characteristics of Ba–W dispenser cathode doped with spray-dried nano-sized scandia. Chin J Vac Sci Technol. 2015;35(12):1431.
87. Wang JS, Cui YT, Liu W, Zhang XZ, Wang YM, Zhou ML. Preparation and emission property of scandia doped tungsten pressed cathode. 7th national conference on functional materialsand applications. Changsha, China. 2010. p. 329.
88. Li LL, Wang JS, Zhao L, Liu W, Wang YM, Zhou ML. Study on scandia mixed matrix impregnated cathode in microstructure and properties. Chin J Rare Met. 2006;30:1.
89. Li L, Wang Y, Wei L, Wang Y, Wang J, Srivastava A, So JK, Park GS. Development of high-current sheet beam cathodes for Terahertz sources. IEEE Trans Electron Devices. 2009;56(5):762.
90. Cui Y, Wang J, Liu W, Wang Y, Zhou M. Characterization of scandia doped pressed cathode fabricated by spray drying method. Appl Surf Sci. 2011;258(1):327.
91. Wang J, Wang Y, Liu W, Li L, Lu H, Wang Y, Li H, Yang J. High current density scandia doped pressed cathode and shaped beam generation. 8th IEEE international vacuum electronics conference (IVEC). Kitakyushu, Japan. 2007. p. 243.

92. Sasaki S, Yaguchi T, Nonaka Y, Taguchi S, Shibata M. Surface coating influence on scandate cathode performance. Appl Surf Sci. 2002;195(1–4):214.
93. Yamamoto S, Taguchi S, Watanabe I, Sasaki S. Electron emission enhancement of a (W-Sc_2O_3)-coated impregnated cathode by oxidation of the coated thin film. Bus Horiz. 1988;32(6):24.
94. Wright DA, Woods J. The emission from oxide-coated cathodes in an accelerating field. Proc Phys Soc. 1952;65(2):134.
95. Raju RS, Maloney CE. Characterization of an impregnated scandate cathode using a semiconductor model. IEEE Trans Electron Devices. 1994;41(12):2460.
96. Wang Y, Wang J, Liu W, Zhang K, Li J. Development of high current-density cathodes with scandia-doped tungsten powders. IEEE Trans Electron Devices. 2007;54(5):1061.
97. Zhang X, Wang J, Wang Y, Liu W, Zhou M, Gao Z. Investigation of influence of surface nanoparticle on emission properties of scandia-doped dispenser. Funct Mater Lett. 2013;6(4):1350040.
98. Vlahos V, Lee YL, Booske JH, Morgan D, Turek L, Kirshner M, Kowalczyk R, Wilsen C. Ab initio investigation of the surface properties of dispenser B-type and scandate thermionic emission cathodes. Appl Phys Lett. 2009;94(18):184102.
99. Kapustin VI, Li IP, Shumanov AV, Lebedinskii YY, Zablotskii AV. Physical operating principles of scandate cathodes for microwave devices. Tech Phys. 2017;62(1):116.
100. Liu X, Zhou Q, Maxwell T, Vancil B, Beck MJ, Balk TJ. Scandate cathode surface characterization: emission testing, elemental analysis and morphological evaluation. Mater Charact. 2019;148:188.

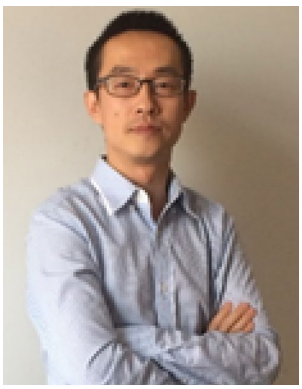

Dr. Peng Hu is currently a professor at Materials Science and Engineering, Beijing University of Technology. He received his B. S. degree from Beijing University of Chemical Technology in 2000, and obtained his Ph.D. degree from Institute of Process Engineering (IPE), Chinese Academy of Sciences (CAS) in 2008. From 2012 to 2013, he worked as a Research Fellow at Nanyang Technological University. He joined Beijing University of Technology at 2017 after working 17 years in IPE. His research interests focus on plasma enhanced chemical process, aiming to develop new strategy for large-scale synthesis, structure control and functionalization of nanomaterials for advanced applications.

Dr. Jin-Shu Wang is a professor of Materials Science and Engineering in Beijing University of Technology (BJUT). She received her Ph.D. degree from the College of Materials Science and Engineering, BJUT, in 1999. From 2002 to 2004, she had worked as a postdoctoral researcher in Tohoku University, Japan. Her research interests include refractory metal-based electronic emission materials, renewable energy and environmental materials. She has published over 200 peer reviewed journal (*Adv. Funct. Mater.Appl. Catal. B: Environ.J. Mater. Chem. A*, ect.) papers and 2 books. She has authorized over 40 invention patents of China and 2 American invention patents. She obtained the National Nature Science Fund for Distinguished Young Scholars in 2012. She was awarded the Distinguished Professor of Chang Jiang Scholars Program by the Ministry of Education, China in 2015. She is a senior committee member of Vacuum Electron Society, Chinese Electronics Society, a committee member of Chinese Corrosion & Protection Society, a member of Society of Metallurgical Physicochemistry, and a member of Photocatalysis Industry Association of China. She is also an editor of journals of *Powder Metallurgy Technology, Tungsten, Vacuum electronics Technology*, ect.